www.arpnjournals.com

GROUND PENETRATING RADAR A TOOL TO MAP THE SEISMICALLY INDUCED FAULT AND FRACTURE IN THE COASTAL CLIFF OF EAST COAST OF PORT BLAIR, ANDAMAN

P. Prasad, N. Ramanujam, A.Vignesh, S. H. K. Murti, Qazi Akhter Rasool, S. K. Biswas, Chandrakant Ojha
and A. J. Boopalan
Department of Disaster Management, Pondicherry University, Port Blair, India
Email: toprasad@hotmail.com

ABSTRACT

Frequency of Earthquake-induced landslides or "seismic landslides", are increasing in recent years throughout the world and mounting grim situations due to the heavy damages caused. Seismic shaking produced additional inertial loading on normal stable slopes and triggered landslides and also reactivating dormant landslides. The 26 December 2004 Sumatra-Andaman earthquake with magnitude Mw 9.3 caused uplift in western and submergence in eastern part of entire island system of Andaman and Nicobar and also instigated subsidence, ground deformations and landslides, in the interior part of the islands and also along the coastal regions of Andaman Islands. Coastal landslides or water front landslides occurred in many parts of Islands. An attempt is made to bring out the triggering instant of earthquake-induced coastal landslides along the coastal cliff section in the Eastern part of Port Blair to a distance of three km. through the geophysical technique Ground Penetrating Radar. The coastal landslides cropped up in the wave front exhibit vertical or near-vertical rock faces to heights of up to 15-20 m from mean sea level in the coastal. Those Coastal landscapes typically consist of an alternate layers of clay, silt and sandstone formations of Andaman flysch deposits. The seismic shaking has initiated widespread ground fractures and cracks it dissipates seismic energy due to acceleration of cliff section. Mapping of the lateral and depth wise extension of the internal failure structures in vertical and horizontal discontinuities in the subsurface in the promontory of sea cliff were mapped through Ground Penetrating Radar (GPR) to identify the intersection of discontinuities oriented in N-S and E-W and demarcated as risk zone.

Keywords: ground penetrating radar, seismic coastal landslides, fracture, Andaman.

INTRODUCTION

Frequency of Earthquake-induced landslides or "seismic landslides", are increasing in recent years throughout the world and mounting grim situations due to the heavy damage caused. Earthquake-induced landslides are one of the most damaging natural disasters. Commonly, damage from earthquake-induced landslides is sometime worse than damage related to the shaking and rupture of the earthquake itself. Seismic induced landslides damage and destroy homes and other structures, block roads, destroy utilities, and dam up river and streams. After study of landslides triggered by the 1989 Loma Prieta earthquake (Moment magnitude - Mw 6.9), Keefer (Keefer 2000) pointed out that regional-scale variations in the hazard level of seismically induced landslides might be better correlated with the geological and geomorphologic characteristics rather than the geotechnical parameters. The study of the internal parameters such as internal friction and cohesion did not explain the distribution and density patterns of earthquakes as in the case history of California earthquake (1989), Chi-Chi earthquake of Taiwan (1999), Chuetsu earthquake of Niigata Prefecture, Japan (2004), and Kashmir earthquake of Pakistan (2005). Further, the study indicates that earthquake-induced landslides are resulted from intense shaking in elevated regions of rugged topography. It has been reported that buildings on crests suffer more damage than those located at the base and they conclude that there is always significant amplification of frequencies corresponding to wavelengths about equal to mountain width at hilltops with respect to the base (Geli *et al*., 1988). Similarly, an amplification and de-amplification pattern on slopes leads to a differential energy distribution pattern on the upper part of the slope. For the case of the Chi-Chi earthquake Lin *et al*., (2003) mentioned that landslide frequency is much higher on the crests of hills. Field experiments (Chávez *et al*., 1996; Bouchon *et al*., 1996) indicate that a topographic amplification of seismic energy occur at the top of hills.

Seismic events produce additional inertial loading, which may trigger landslides on normal stable slopes and also reactivate the dormant pre-existing landslides. The disruption of coastal cliff areas by landslides will inhibit the response to the damage and interruption from strong ground shaking and tsunami waves. Seismically-induced landslides are common phenomena produced by medium to large magnitude earthquakes. Landslides can occur more than hundred kilometers away from the epicentre and can influence several hundred and thousand square kilometers. Areas prone to seismically triggered landslides are akin to other landslide prone area. As with the other ordinary landslides, seismically triggered landslides are more friable when soils are saturated with water.

THE STUDY AREA

The Andaman - Nicobar Ridge (ANR) consist of a narrow broken chain of 572 picturesque islands, islets, and rocks extending along a general north-south direction between 14° N and 6.5°N latitude in the south eastern part

of the Bay of Bengal. These Islands (Gokarn *et al*., 2006) as well as several sea mounts are a part of the regional tectonics in the adjoining Bay of Bengal and Andaman Sea, resulting from the north-ward drifting of the Indian plate and its anticlockwise rotation, subsequent to the collision with the Eurasian Plate (Curray *et al*., 1982). This region is the transition zone connecting the Burmese Arc to the north and the Indonesian arc to the south. The tectonic evolution in the ANR and surroundings was initiated during the Cretaceous although the uplift of the ANR is known to have occurred much later, during the Eocene (Karunakaran *et al*., 1968). This region is still tectonically active and classified as V seismic zone, in the outside of the Himalayan belt as evidenced by the several earthquakes of magnitudes in excess of 8 on the Richter scale and the intense vertical movements of the islands and sea mounts witnessed here over the past about 200 years (Bilham *et al*., 2005). Frequent earthquakes with different magnitude along the boundary of Andaman - Sumatra have nurtured the other natural hazards such as tsunami and landslides in recent years.

The great earthquake occurred on 26th December 2004 in Sumatra was responsible for the subsidence of landforms up to 1 to 1.5 m in the eastern part of the south Andaman especially south east part of Port Blair (Malik *et al*., 2006). Seismically triggered landslides are widespread phenomena within tectonically active mountain ranges and generated the landslides in the interior and along the coastal area of the islands. Most of these slope failures are reported to be of smaller in size, such as rock or soil falls, and only a few of them have affected large volumes of soil or rock material. The coastal structures of east coast Andaman Islands are sedimentary form with steep cliff. When the seismic waves hit the coastal land, the cliff sections slacken off the slope stability instantly and down slope movement of cliff mass occurred. Landslide and rock falls incidences are common at the time of heavy rainfall without seismic influence in the islands system. The seismic events very often triggered the unstable soils movements and generated landslides, rock falls or similar events. On the other hand crustal earthquakes with a magnitude greater than 6.0 always more often triggers landslides. The study area in the east part of Port Blair form a narrow protruding landmass between Carbin's coves to Sinclair cliff is composed of Andaman flysch deposits of Oligocene age (Karunakaran, 1968). Coastal cliff area consists of an alternate layers of clay, silt and sandstone formations of Andaman flysch deposits. The vertical or near-vertical rock faces in the coastal cliff area rising from the water front of the sea to as high as 15 to 20 m above mean sea level. The shoreline in this part of area is steep slope with stratified sedimentary beds and trending N15°E; S15°W direction and inclined steeply and dipping towards East. The sea cliff in this area was submerged 1.5 m at the time of the great earthquake in 2004 has increased the wave induced erosion at the base of the cliff area. Nevertheless, peak ground acceleration of the great earthquake with high magnitude of 9.2 is also competent of producing such sea cliff failure (Ramanujam

et al., 2010). It is evident from the field that such large earthquake has caused instantaneous cliff retreat and also weaken sea cliff through seismic shaking and formed cracks and fissures, thereby increasing the vulnerability of the cliff section to subsequent failure (Prasad and Ramanujam, 2012). Due to these factors the promontories in the study area are consistently the sites for the extensive slope failures.
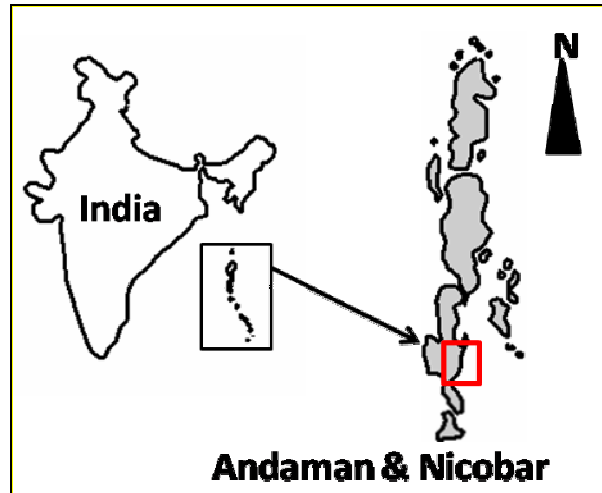
Figure-1. Study area.

METHODOLOGY

Various types of Geophysical techniques are being applied to study the landslides with slopes from few degrees to vertical to a depth of 400 m (Ramanujam *et al*., 2008). Aims of the geophysical surveys are to map the internal structure of the landslides or to locate the vertical and lateral boundaries of the slip zone of the failure surface.

A number of publications of case studies using GPR data have been increased considerably during the last ten years. The success is due to; 1) high resolution, range of antenna frequencies from a few cm to a few m; 2) wide range of penetration depth in resistive materials; 3) sensitivity to dielectric, electric and magnetic contrast and particularly to water content, and; 4) its light instrumentation. All of these properties make it potentially appropriate for investigations in various fields (geological, geomorphological, glaciological, environmental, geotechnical, hydrological). However, severe limitations decrease this potential for landslide investigations, as attested by the very low number of applications in this field. First, GPR signals are highly attenuated in high conductive formations, thus preventing any application in soil landslides or when water saturation is higher than the target. Second, heterogeneities like fractures and blocks create diffractions, decrease the penetration depth dramatically. Bichler *et al*. (2004) studied landslides using low-frequencies with 50 MHz antennas and presented GPR reflection profiles and identified several radar facies to a depth of 25 m to detect possible slip surface. Internal structure of two large seismically induced landslides in

Anchorage (Alaska) and subsurface geometry of horst and graben structures down to a depth of 10 m are imaged through GPR by Barnhardt and Kayen (2000). The presence of electrically conductive clay deposits at greater depth reduces penetration depth made impossible to image the failure surface. Applications of field investigations of rock fall, slope stability assessment have been favoured by the high resolution properties and penetration depth in resistive formation through GPR. Jeannin *et al*. (2006) evaluated the potential of discontinuities on a limestone cliff and reached a maximum penetration of 20 m GPR measurements with reflection, CMP, tomography configurations with 100 MHz antenna.

Ground penetrating radar survey

The GSSI -3000 GPR system with 35 MHz frequency, with bistatic separate transmitter and receiver antenna are used for the present study. The transmitter produces a short duration, high voltage pulse transmitted through the transmitter antenna, which in turn radiates an electromagnetic signal into the ground. The reflected signal travels back to the receiver antenna and recorded as an amplitude trace. The antenna recording was point mode along the cliff following the horizontally orientation of the scan line measurements. Six GPR survey measurements were carried out with two-way travel time setting of 500 ns per 1024 samples per scan. Measurements were conducted with the additional of markers every 3 m during data acquisition. This marker was then used to estimate the position of measurements across the horizontal measurements.

Table-1. The antenna parameters.

Profile	I	II	III	IV	V	VI
Antenna (MLF)	35 MHz	35 MHz	35 MHz	35 MHz	35 MHz	35 MHz
Antenna length	3.6 m	3.6 m	3.6 m	3.6 m	3.6 m	3.6 m
Profile direction	E-W	NNE-SSW	NE-SW	NE-SW	SE-NW	N-S
Distance between Tx and Rx antennas	2 m	3 m	3 m	3 m	3 m	3 m
Length of each profile	40 m	54 m	54 m	42 m	81 m	84 m
Depth	30 m	30 m	30 m	30 m	30 m	30 m

GPR data processing

GPR datasets were processed by using RADAN 6 software. The processing procedure was a standard one for typical GPR data; i) Horizontal scale adjustment- Distance normalization to establish a constant horizontal scale between the marks, equal number of scans per unit distance between marks. ii) Horizontal scaling- stretching function to expand the horizontal scale, vertical scale adjustments to adjust the position of the whole profile in the data window (adjust time zero), surface normalization to correct the elevation changes. iii) Automatic gain ontrol (AGC) was carried out, to compensate for the attenuation of the late arriving EM waves. This allowed some of the deeper reflections to be seen. iv) Background removal was applied to remove the noise that masks the reflection events of interest. v) A band pass filter was applied to improve the signal/noise ratio. This algorithm reduces diffraction hyperbolas down to a single point and collapse the dipping event to their true orientation. The period of antenna ringing is determined by the amount of time required for currents to travel between the antenna feed and ends of the antenna elements, whose velocity depends on the antenna design (Radzevicius *et al*., 2000). Change of colour transform to enhance weak amplitude or small contrast reflectors. The intensity value that represents the amplitude reflections of the discontinuities may vary due to variation in in-fill material, aperture, and degree of weathering of reflecting discontinuities. This implies that different linear features corresponding to particular

discontinuities have a varying intensity values. In view of this, the threshold set for extreme intensity change delineation were also varied based on the assessment of the intensity profile as discussed above. The likely intensity change corresponding to a linear event can be assessed, first by visual inspection of the intensity profile of the image. The proposed discontinuity detection algorithm for Ground Penetrating Radar (GPR) data discontinuity measurements helps in objectively delineating the linear coherent events, amidst the presence of high amplitude, non-coherent reflections.

RESULTS

The first GPR profile taken in the E-W direction perpendicular to coastal cliff towards landwards to distance of 40 m this show the features of crumbling bed at 10 m, the fissure and vertical fractures traced with white dotted line down to 25m in the time slice profile (Figure-2(a)). Due to presence of fresh water in fractured zones the electromagnetic waves are attenuated and some parts of beds are not clearly seen. The second GPR profile taken in NNE-SSW direction in the intertidal zone to the distance of 54m exhibit attenuation of electromagnetic waves along the fault boundary and bedding plane up to the depth of 10 m obscured the bedding nature (Figure-2(b)). Vertical and inclined fractures are seen in the profile delineate with white dotted line. The third and fourth GPR profile taken in NE - SW direction to the vicinity of Megapod resort in the intertidal coastal zone to the distance of 96 m (Figure-

2(c) and (d)). Vertical and inclined fractures are seen in the profile. The fractures zone produces the scattering of electromagnetic wave due to the saturated with salt water, this may attenuate the GPR signals, causing decreased amplitude over this zone.
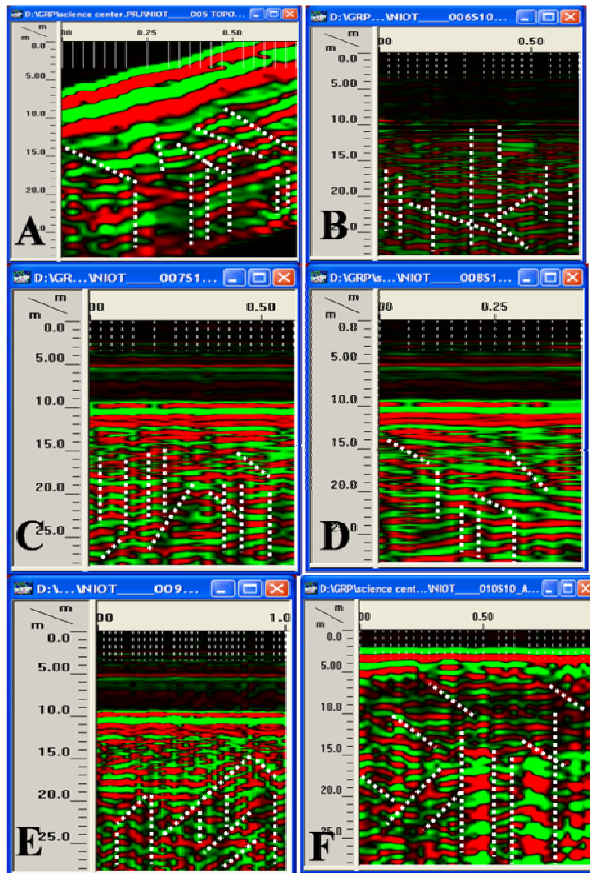
Figure-2. GPR profile.

The fifth GPR profile section was survey in NW-SE direction in the intertidal coastal zone to the distance of 81 m (Figure-2(e)). These transect show a chaotic reflection patterns in the depth of 15 m. This chaotic reflection pattern is most prominent. This irregular reflection pattern can be explained by an irregular subsurface structure, possibly due to ground seismic shaking. The penetration of radar signal is less because radar wave attenuation was strongly dependent on the electric conductivity function the lower radar penetration bind with the high electrical conductive (high dielectric constant) that were found in this area. The sixth GPR profile section was survey in N-S direction in the intertidal coastal zone to the distance of 84 m. (Figutre-2(f)) this transects exhibit attenuation of electromagnetic waves along the fault boundary and bedding plane up to the depth of 15 m, obscured the bedding nature. Vertical and inclined fractures are seen in the profile.
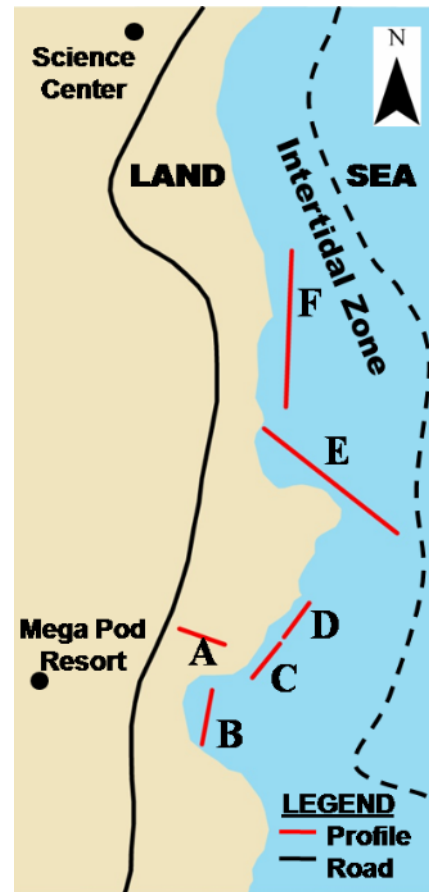
Figure-3. Survey line of GPR profile.

DISCUSSIONS

Detection and mapping of fracture orientation and fracture density were computed after processing all GPR data in Radar 6 Software. Application of the maximum curvature attribute localizes the response of the fractures in the volume. The linear patterns appear even more clearly in each time slices, and for each the measured fracture directions in the rose diagram appear as high amplitude lineation on the time slices. All four directions in the rose diagram are represented in the lineation. In the Figure-4 (a), rose diagram exhibit the fracture orientations retrieved from GPR profile taken in E-W direction perpendicular to the coast cliff section. In Figure-4 (b), rose diagram exhibit the fracture orientations retrieved from GPR profile taken in NNE-SSW direction. In Figure-4 (c), rose diagram exhibit the fracture orientations retrieved from GPR profile NE - SW direction in the coastal zone. In Figure-4 (d), rose diagram exhibit the fracture orientations retrieved from GPR profile NE -SW direction. In Figure-4(e), rose diagram exhibit the fracture orientations retrieved from GPR profile NW - SE direction. In Figure-4 (f), rose diagram exhibit the fracture orientations retrieved from GPR profile N - S direction in the coastal zone. Interestingly, the most populous fracture direction (yellow in the rose diagram) is represented in GPR profiles. Particular directions seem to be localized in

different sectors of the time slice, so a future task is to subdivide the fractures represented in the rose diagrams into outcrop locations where they were measured.
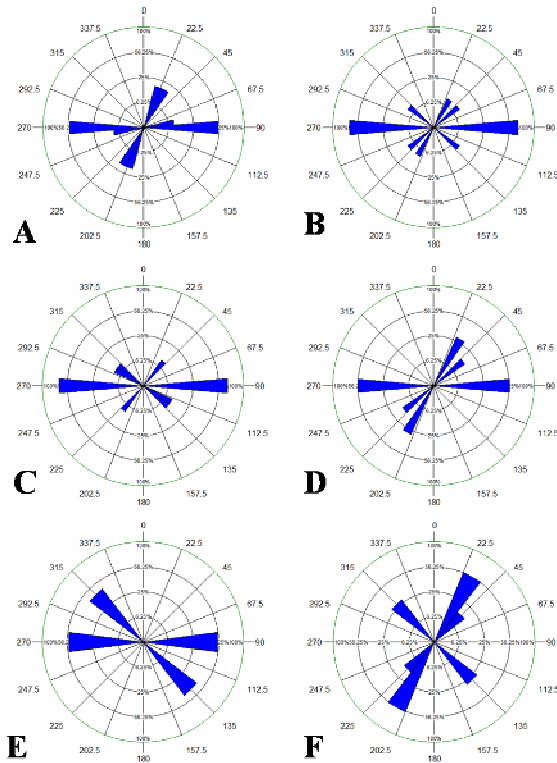
Figure-4. Fracture orientation
in rose diagram of each profile.
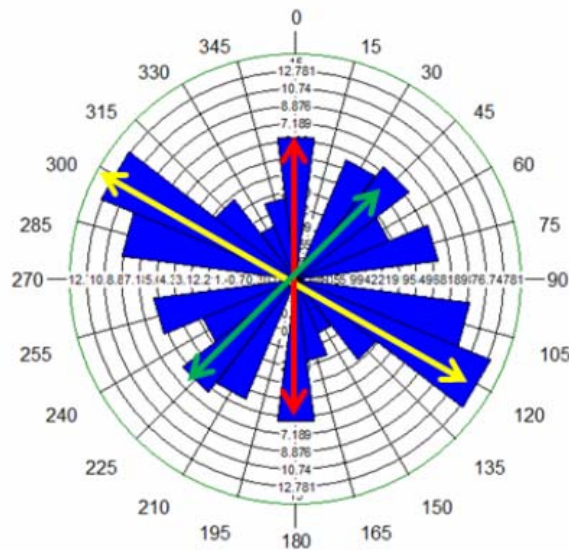
Figure-5. Major fracture orientation in
rose diagram.

CONCLUSIONS

This Andaman region is still tectonically active as evidence by the several earthquake of magnitude in excess of 8 on the Richter scale and the intense vertical movement of the island and sea mount witnessed here the past about 200 years. (Bilham *et al*., 2005). The Ninety East Ridge is a complex zone of deformation within the Indian plate and part of the ridge experienced intense seismic activity in the past. The seismicity is concentrated in a zone paralleling the ridge, on its northern segment. Its northern portion (up to 10°S) is seismically more active and undergoing NW-SE compression, wherein both vertical as well as strike slip motions occur. The GPR clearly imaged the internal structure of landslide, fault, fracture caused by the 2004 Andaman - Sumatra and past earthquake. The profile carried out perpendicular and parallel to the cliff section and intertidal zone revealed many structural discontinuities such as fault, fractures, folding in study area creating owing to the seismic shaking. GPR has vast utility in evaluating landslide zone and to assess fracture density in a rapid non-destructive manner. Rose diagrams of lineament trends (Figure-5) reveal from the GRP image that the majority of lineaments fall into clusters with orientations of NW- 40 and SE - 40.

REFERENCE

Barnhardt W.A and Kayen R.E. 2000. Radar structure of Earthquake induced coastal landslides in Anchorage, Alaska. Environmental Geosciences. 7(1): 38-45.

Bichler A, Bobrowsky P, Best M, Darma M, Hunta J, Calvert T and Burn R. 2004. Three dimensional mapping of a landslide using multi geophysical approach: The Quesnel Forks landslide, Landslide. 1(1): 29-40.

Bilham R., E. R. Engdhal, N. Feldl and S. P. Satyabala.2005. Partial rupture of the Indo-Andaman plate boundary 1847-2004, Seism. Rev. Lett. (Downloaded from the web site, http://cires.colorado.edu).

Bouchon M, Schultz CA and Toksoz MN. 1996. Effect of three-dimensional topography on seismic motion. Journal of Geophysical Research. 101(B3): 5835-5846.

Chávez-García FJ, Sanchez LR and Hatzfeld D. 1996. Topographic Site Effects and HVSR, A Comparison between Observation and Theory. Bulletin of the Seismological Society of America. 86(5): 1559-1573.

Curray J. R., F. J. Emmel, D. G. Moore and R. W. Raitt. 1982. Structure, tectonics and geological history of the north eastern Indian ocean, in Ocean basins and margins. E. M. Nairn and F. G. Stehli (Ed.). Plenum, New York. 6: 399-450.

Geli L, Bard PY and Jullien B. 1988. The effect of topography on earthquake ground motion: review and new results. Bulletin of the Seismological Society of America. 78(1): 42-63.

Gokarn S. G., Gautam Gupta, Shipra Dutta and Nitu Hazarika. 2006. Earth Planets Space. Geoelectric structure in the Andaman Islands using magnetotelluric studies. 58: 259-264.

Jeanning M, Garmbis S, Gregoire S and Jongmans D. 2006. Multi-configuration GPR measurements for geometrical fracture characters in limestone cliff (Alps) Geophysics. 71: 885-892.

Karunakaran C. K., K. Ray and S. S. Saha. 1968. A new probe in to the tectonic history of the Andaman and Nicobar islands. 22nd International Geol. Congr., India.

Keefer DK. 2000. Statistical analysis of an earthquake-induced landslide distribution - the 1989 Loma Prieta, California event, Engineering Geology. 58(3-4): 231-249.

Lin C-W, Shieh C-L, Yuan B-D and Shieh Y-C Liu S-H Lee S-Y. 2003. Impact of Chi-Chi earthquake on the occurrence of landslides and debris flows: example from the Chenyulan River watershed, Nantou, Taiwan, Engineering Geology. 71: 49-61.

Malik J.N, Murty C.V.R, Eeri M and Ravi R. 2006. Landscape changes in Andaman and Nicobar islands (India) after December, 2004 Great Sumatra Earthquake and Indian Ocean Tsunami. Earthquake Spectra. 22(S3): 43-66.

Prasad P and Ramanujam N. 2012. A study of seismically induced coastal landslides in south eastern part of port Blair, south Andaman through remote sensing and GIS Indian Landslide. 5(1): 35-42.

Ramanujam N, Antony Ravendran, Kannan, Baby Meena Losini and Udayana Pillai A.V. 2008. Resistivity tomographic Imaging study of some landslides in Ooty area, Niligiris District, Tamil Nadu. 1(2): 37-50.

Ramanujam. N, Dharanirajan. K, Mothilal Yuvaraja. P and Prasad. P. 2010. A study of rock slope failures in the coastal Landslide zone in the south eastern part of Port Blair through Ground penetrating radar and Resistivity imaging techniques. Indian landslides. 3(1): 1-8.

Radzevicius. S., Guy. E and Daniels. J. 2000. Pitfalls in GPR data interpretation: differentiating stratigraphy and buried objects from periodic antenna and target effects. Geophysical Research Letters. 27(20).